X71-72135

A Reproduced Copy

OF

Rm SA 53G08

Reproduced for NASA

by the

NASA Scientific and Technical Information Facility

FFNo 672 Aug 65

AUG 26 1953 REC'D

AUG 31 1953 REC'D

14 total

[redacted]

Copy 1

RM SA53G08

NACA RM SA53G08

Declassified by authority of NASA
Classification Change Notices No. ~~2 1 2~~
Dated ** ~~31 MAR 1971~~

TD 71-36
12-14-70

NACA

[redacted]

RESEARCH MEMORANDUM

for the

United States Air Force

WIND-TUNNEL INVESTIGATION OF THE DRAG AND LATERAL-STABILITY CHARACTERISTICS OF A 1/22-SCALE MODEL OF A BOMBER AIRPLANE EMPLOYING A LOW-ASPECT-RATIO TRIANGULAR WING

By E. Ray Phelps

Ames Aeronautical Laboratory
~~Moffett Field, Calif.~~

CLASSIFICATION CHANGE
To Unclassified
By authority of CCN # 7359
Changed by H. G. Hannah Date 12-15-70

CLASSIFICATION CHANGED
UNCLASSIFIED
TO
By Authority of NASA TD 71-36 Date 12/15-70

Authority NACA RESEARCH ABSTRACT
Classification Notice No. 122

Date 12/3/57

[redacted]

NATIONAL ADVISORY COMMITTEE FOR AERONAUTICS

WASHINGTON

July 8, 1953

141

 [redacted]

NATIONAL ADVISORY COMMITTEE FOR AERONAUTICS

RESEARCH MEMORANDUM

for the

United States Air Force

WIND-TUNNEL INVESTIGATION OF THE DRAG AND LATERAL-STABILITY CHARACTERISTICS OF A 1/22-SCALE MODEL OF A BOMBER AIRPLANE EMPLOYING A LOW-ASPECT-RATIO TRIANGULAR WING

By E. Ray Phelps

SUMMARY

This report presents the results of a wind-tunnel investigation of the effect of model cross-sectional-area distribution, nacelle configuration, and landing-gear-fairing configuration upon the minimum-drag characteristics of a 1/22-scale model of a four-engined bomber airplane employing a low-aspect-ratio triangular wing. The drag characteristics were shown for Mach numbers from 0.7 to 0.9 and from 1.4 to 1.9. The lateral-stability characteristics were also investigated for the model with various nacelle configurations at Mach numbers of 1.4 and 1.9. All data were obtained at a Reynolds number of 3.0 million based upon the wing mean aerodynamic chord.

The effectiveness of a modification made according to the transonic-area rule could not be investigated at transonic speeds; however, at Mach numbers below 0.9 and above 1.4 the modification increased the drag. This drag increase appeared to be associated with abrupt changes in body contour since a revision, which reduced the abruptness of these contour changes, resulted in significant drag reduction in the Mach number range of this investigation. The results of the investigation of the effect of nacelle configuration indicated substantially less drag for the arrangement with outboard nacelles centrally located in the wing. The drags attributable to three types of landing-gear fairings were approximately the same. A reduction in directional stability resulted from the addition of the nacelle configurations investigated.

[redacted]

INTRODUCTION

The results of recent experiments have shown that the drag caused by the effects of interference between various components of an airplane can become excessive at transonic and supersonic speeds. Although these results have indicated design criteria to be followed in order to reduce the adverse effects of interference, the accurate prediction of such effects is difficult. At the request of the U. S. Air Force, tests have been conducted in the Ames 6- by 6-foot supersonic wind tunnel to determine the drag characteristics of a 1/22-scale model of a bomber-type airplane employing a triangular wing of aspect ratio 2.3. These tests were directed principally toward measuring the drag changes resulting from an application of the transonic-area rule and toward investigating the effects upon over-all drag of several nacelle configurations and other wing-mounted appendages. In conjunction with the drag investigation, an experimental study of the effect of nacelle configuration upon the lateral-stability characteristics of the model was made.

NOTATION

A	cross-sectional area of model in planes perpendicular to the longitudinal axis, sq in.
A_e	exit area of one nacelle, sq in.
b	wing span in chord plane, in.
$\bar{c}$	wing mean aerodynamic chord, in.
$C_{D_{min}}$	minimum-drag coefficient, $\frac{\text{minimum drag}}{qS}$
C_{D_i}	nacelle internal-drag coefficient, $\frac{\text{internal drag}}{qS}$
C_Y	side-force coefficient, $\frac{\text{side force}}{qS}$
C_n	yawing-moment coefficient, $\frac{\text{yawing moment}}{qSb}$
C_l	rolling-moment coefficient, $\frac{\text{rolling moment}}{qSb}$
l	model length, in.
m	mass rate of flow through one nacelle, slugs/sec

p_o free-stream static pressure, lb/sq in.

p_e nacelle exit static pressure, lb/sq in.

q free-stream dynamic pressure, lb/sq in.

S total wing area in chord plane, including area formed by extending leading and trailing edges to model plane of symmetry, sq in.

V_o free-stream velocity, ft/sec

V_e nacelle exit velocity, ft/sec

β angle of sideslip of fuselage longitudinal axis, deg

APPARATUS

Wind Tunnel and Equipment

The experimental investigation was conducted in the Ames 6- by 6-foot supersonic wind tunnel. In this wind tunnel, the Mach number can be continuously varied from 0.60 to 0.90 and from 1.15 to 2.00, and the stagnation pressure can be regulated to maintain the desired test Reynolds number.

The model was mounted on a sting having a cross-sectional area of 48 percent of the base area of the model. Aerodynamic forces and moments were measured by means of a six-component, flexure-pivot-type strain-gage balance mounted in the body of the model.

Model

A 1/22-scale model of a four-engined bomber-type airplane consisting of two separable units, a return component and a pod, was used in the present investigation. A photograph of the model is shown in figure 1 and a three-view drawing in figure 2.

The return component consisted of a flat-bottomed body mounting a triangular wing of aspect ratio 2.3 and a sweptback vertical tail. The wing had an NACA 0004.5-64 airfoil section in streamwise planes perpendicular to the chord plane and was mounted on the body with 3.0° incidence and 2.2° negative dihedral. Provision was made for attaching several ducted nacelles and other appendages on the wing.

The pod had a flat top for attachment beneath the return component to complete the composite configuration. Two small triangular wings and a sweptback vertical tail were mounted on the pod for control during separated flight.

The nacelle configurations included in the present investigation consisted of the following:

(1) Split nacelles

Inboard nacelles pylon mounted under the wing in conjunction with outboard nacelles mounted over the wing (fig. 3(a))

(2) Split nacelles, outboard nacelle on chord plane

The same inboard nacelles as (1) with the outboard nacelle submerged in the wing (fig. 3(b))

(3) Siamese nacelles

Two nacelles mounted in Siamese arrangement under each wing panel (fig. 3(c))

(4) Siamese nacelles with center bodies

The Siamese arrangement of (3) with a probe and center body faired between each pair of inlets (fig. 3(c))

The aforementioned appendages on the wing were streamlined fairings, shown in figure 4, simulating landing-gear housings. Three types of these fairings were provided: (1) an under-wing fairing mounted at the 15-percent semispan station, (2) an over- and under-wing fairing at approximately the same location, and (3) an over- and under-wing fairing mounted at approximately 23-percent semispan.

A modified composite configuration had a higher model fineness ratio[1] and a more gradual longitudinal progression of model cross-sectional area[2] than the original configuration. This modification

---

[1]Model fineness ratio is defined as the fineness ratio of an equivalent body of revolution having a length equal to that of the model and a maximum cross-sectional area equal to the maximum model cross-sectional area.

[2]Model cross-sectional area includes the cross-sectional area in a given plane perpendicular to the body reference axis of all components of the model.

was accomplished by lengthening and recontouring the body and pod and relocating the nacelles and vertical surfaces. The original and modified configurations, with the nacelles omitted for clarity, are compared in figure 2. The modified composite configuration utilized the split-nacelle arrangement with the outboard nacelles moved rearward 2.27 inches from the position shown in figure 3(a).

TESTS AND PROCEDURE

Range of Test Variables

The drag characteristics of the composite model with several nacelle and landing-gear-fairing configurations, the modified composite model, and the return component (composite model minus pod) were investigated through a limited angle-of-attack range at Mach numbers of 0.7, 0.8, 0.9, 1.4, 1.6, 1.75, and 1.9. The lateral characteristics of the composite model with several nacelle configurations were investigated at nominally zero angle of attack at Mach numbers of 1.4 and 1.9. All tests were conducted at a Reynolds number of 3.0 million based upon the wing mean aerodynamic chord.

Reduction of Data

The data presented herein have been reduced to standard NACA coefficient form based upon the total wing area in the chord plane, including the area formed by extending the leading and trailing edges to the plane of symmetry. These coefficients were referred to the stability axes with the origin located longitudinally at a position corresponding to 37 percent of the mean aerodynamic chord and 0.182 inch above the parting plane between the return component and the pod. Factors which could affect the accuracy of the results, together with the corrections applied, are discussed in the following paragraphs.

Tunnel-wall interference.- At subsonic speeds the effects of constriction of the flow around the model due to the presence of the tunnel walls were accounted for by the method of reference 1. At supersonic speeds, the reflection from the tunnel walls of the shock wave originating at the nose of the model did not cross the model; no corrections were required, therefore, for tunnel-wall effects.

Stream variations.- Previous investigations in the 6- by 6-foot wind tunnel have indicated a significant curvature of the air stream in a vertical plane in the test section but little or no curvature in a horizontal plane. The effects upon a model of these stream variations were shown in reference 2 to be minimized by confining the pitch and yaw planes of the model to the horizontal plane. This procedure was followed throughout the present test.

To determine the effects of stream curvature on the model of this investigation, the model was tested in the normal attitude and also rolled 180° on its longitudinal axis. The results of these tests showed negligible effects upon the minimum drag of the model; the principal effect was a translation from the origin of the lateral-stability curves presented herein. The data presented were obtained with the model in the normal attitude and were not corrected for stream-angle effects.

In reference 2, a static-pressure gradient of sufficient magnitude to affect the drag results was shown to exist along the longitudinal axis of the test section. A correction was made to the measured drag, therefore, to account for the longitudinal force caused by this static-pressure variation.

Internal nacelle drag.- The drag data presented herein do not include the internal drag of the nacelles. The internal-drag coefficients were calculated from

$$C_{D_i} = \frac{m\,(V_o - V_e) + Ae\,(p_o - p_e)}{q_o S}$$

where the flow quantities at the nacelle exits were measured by means of pitot-static rakes. These coefficients were subtracted from the measured drag coefficients.

Support interference.- The effects of support interference were shown in reference 3 to be limited, at supersonic speeds, to a change in base pressure for sting-body combinations similar to that of the present test. This fact was substantiated during a previous test in the 6- by 6-foot wind tunnel and was found, for that specific model, to apply also at the subsonic Mach numbers of the present investigation. The assumption was made, therefore, that the effects of support interference were confined to a change in base pressure during the present investigation.

The drag data presented herein were adjusted to conditions of free-stream static pressure at the base of the model and are, therefore, forebody drag coefficients.

Angles of attack and sideslip.- The determination of the actual angles of attack and sideslip of the model under load required that several corrections be made to the calibrated static angles. Corrections were applied to account for the angular deflection of the sting and balance under aerodynamic load and for angular movement due to structural clearances in the model support system.

[redacted]

Precision of Measurements

From consideration of the repeatability of the data and the known uncertainties of the data, the precision of measurements made during the present investigation is estimated to be as follows:

Quantity	Precision
$C_{D_{min}}$	0.0010
C_l	.0008
C_n	.0010
C_Y	.0015
M	.01
R	$.03 \times 10^6$
β	.10

It is estimated that the precision of the incremental drag coefficients is greater than that of the individual measurements, possibly of the order of 0.0005.

RESULTS AND DISCUSSION

Minimum-Drag Characteristics

Effect of cross-sectional-area distribution.- The longitudinal distribution of model cross-sectional area has been shown in reference 4 to be a principal factor in determining the transonic drag-rise characteristics of thin, low-aspect-ratio-wing and body combinations. It was shown that, in general, a decrease in the rate of expansion or contraction of model cross-sectional area resulted in a decrease in the drag rise at Mach numbers near unity. These concepts were therefore applied to the model of the present investigation resulting, as shown in figure 5, in a modified composite model having a smaller maximum cross-sectional area and a greater body length than the original model.

Unfortunately, it was not possible to obtain drag characteristics for these two models in the Mach number range wherein the modifications would be expected to show the greatest benefit, Mach numbers from 0.9 to 1.4. Outside this range, the data of figure 5 indicate no improvement in the minimum-drag (approximately zero-lift drag) characteristics due to the modifications incorporated into the model. On the contrary, the minimum-drag coefficients of the modified composite model were approximately 0.0015 greater than those for the original model throughout the Mach number range of the investigation. The higher minimum-drag coefficients for the modified composite model

are believed to be caused by separation of the boundary layer from the aft portions of the body as a result of the abrupt variations in body contour incorporated into the modified composite model. This fact was indicated during another portion of the investigation wherein the body and pod of the modified composite model were revised to reduce the abrupt variations of body contour. The data from these tests, figure 6, showed that the minimum-drag coefficients were reduced by approximately 0.0025 as a result of the revisions made to the modified composite model. The revision had no effect on the drag rise from a Mach number of 0.9 to 1.4, however. It would appear from these results that the shape of the individual components of an airplane is as important as the variation of model cross-sectional area. Thus, in obtaining a favorable longitudinal distribution of total cross-sectional area, the variation in contour of any component of the airplane must not be so abrupt as to promote separation, and, hence, an increase in drag, over most of its Mach number range. It should be noted that the data of figures 5 and 6 are not comparable because the results shown in the latter figure are for the model without horizontal or vertical surfaces on the pod.

The minimum drag of the return component (fig. 5) is shown to be about 20 percent less than for the composite model. Of this reduction, about one-half at subsonic speeds and one-fifth at supersonic speeds can be attributed to the pod surfaces.

Effect of nacelle configuration.- A comparison of the minimum-drag coefficients for the composite model with various nacelle configurations is given in figure 7. The results show that the various nacelle configurations caused a substantial increase in minimum drag of the model, averaging approximately 45 percent in the Mach number range of this investigation. Of the various configurations investigated, that having outboard nacelles on the chord plane had the lowest drag. The minimum-drag coefficient for this configuration was approximately 9 percent less than that for the other configurations investigated; this is attributed to the better design of the outboard nacelle located on the chord plane. At the attitude for minimum drag, the angle of attack of the nacelle on the chord plane was approximately 0.7°; whereas that of the outboard nacelle mounted above the chord plane was approximately -2.5°. Furthermore, the nacelle-wing juncture of the outboard nacelle on the chord plane contained no re-entrant contours in contrast to that for the other nacelle configurations, thus minimizing nacelle-wing interference.

It should be mentioned that the data in figure 7 were obtained with the model also equipped with the over- and under-wing landing-gear fairings. In the case of the configuration indicated as the composite model with split nacelles, the fairings were at the inboard location; whereas for the remaining configurations the fairings were at the outboard position. As shown in the next section, this difference in arrangement of the landing-gear fairings should have little effect on the results shown in figure 7.

Effect of landing-gear fairing.- Minimum-drag coefficients as functions of Mach number are shown in figure 8 for the model with split nacelles (outboard nacelles mounted over the wing) and various landing-gear fairings. It may be seen that each type of landing-gear fairing produced an average increment of drag of about 6 percent at subsonic speeds and 9 percent at supersonic speeds.

Lateral-Stability Characteristics

The variations of rolling-moment, yawing-moment, and side-force coefficients with sideslip angle for the composite model with several nacelle configurations are shown in figure 9 for Mach numbers of 1.4 and 1.9. Examination of this figure indicates that the directional stability of the model was reduced by the addition of the nacelles. This condition resulted from the fact that the inboard and Siamese nacelles were mounted on the wing forward of the center of moments so that the side force on the nacelles in sideslip reduced the yawing-moment coefficients.

The results of figure 8 show, in several cases, a small moment and side force at a sideslip angle of 0°. This characteristic was due principally to the effects of stream irregularities, as indicated by the results obtained from tests of the model in the normal and inverted attitudes.

CONCLUDING REMARKS

From an analysis of the results of this investigation, the following observations can be made:

1. The effectiveness of a modification made according to the transonic area rule could not be investigated at transonic speeds; however, at Mach numbers below 0.9 and above 1.4 the modification increased the drag. This drag increase appeared to be associated with abrupt changes in body contour since a revision, which reduced the abruptness of these contour changes, resulted in significant drag reduction in the Mach number range of this investigation.

2. The increment of drag due to the nacelles was found to be less for the configuration involving outboard nacelles submerged in the wing.

3. A reduction in directional stability resulted from the addition of each of the nacelle configurations investigated.

Ames Aeronautical Laboratory
National Advisory Committee for Aeronautics
Moffett Field, Calif., July 8, 1953

REFERENCES

1. Herriot, John G.: Blockage Corrections for Three-Dimensional-Flow Closed-Throat Wind Tunnels, with Consideration of the Effect of Compressibility. NACA Rep. 995, 1950. (Formerly NACA RM A7B28)

2. Frick, Charles W., and Olson, Robert N.: Flow Studies in the Asymmetric Adjustable Nozzle of the Ames 6- by 6-Foot Supersonic Wind Tunnel. NACA RM A9E24, 1949.

3. Perkins, Edward W.: Experimental Investigation of the Effects of Support Interference on the Drag of Bodies of Revolution at a Mach Number of 1.15. NACA TN 2292, 1951. (Formerly NACA RM A8B05)

4. Whitcomb, Richard T.: A Study of the Zero-Lift Drag-Rise Characteristics of Wing-Body Combinations Near the Speed of Sound. NACA RM L52H08, 1952.

FIGURE LEGENDS

Figure 1.- The composite model equipped with split nacelles.

Figure 2.- Three-view drawing of the model.

Figure 3.- Details of the various nacelle configurations used on the model. (a) Split nacelles.

Figure 3.- Continued. (b) Outboard split nacelle on chord plane.

Figure 3.- Concluded. (c) Siamese nacelles.

Figure 4.- Details of the landing-gear fairings used on the model.

Figure 5.- The effect of longitudinal cross-sectional-area distribution upon the minimum-drag characteristics of the model with split nacelles. Reynolds number, 3.0 million.

Figure 6.- A comparison of the minimum-drag characteristics of the modified and revised modified composite models without pod surfaces. Reynolds number, 3.0 million.

Figure 7.- Comparisons of the longitudinal cross-sectional-area distributions and the minimum-drag characteristics for the composite model with several nacelle configurations. Reynolds number, 3.0 million.

Figure 8.- The effect of several landing-gear fairings upon the minimum-drag characteristics of the composite model with split nacelles. Reynolds number, 3.0 million.

Figure 9.- Variation of the lateral-stability characteristics with sideslip angle for various nacelle configurations on the composite model at a lift coefficient of 0.08. Reynolds number, 3.0 million.

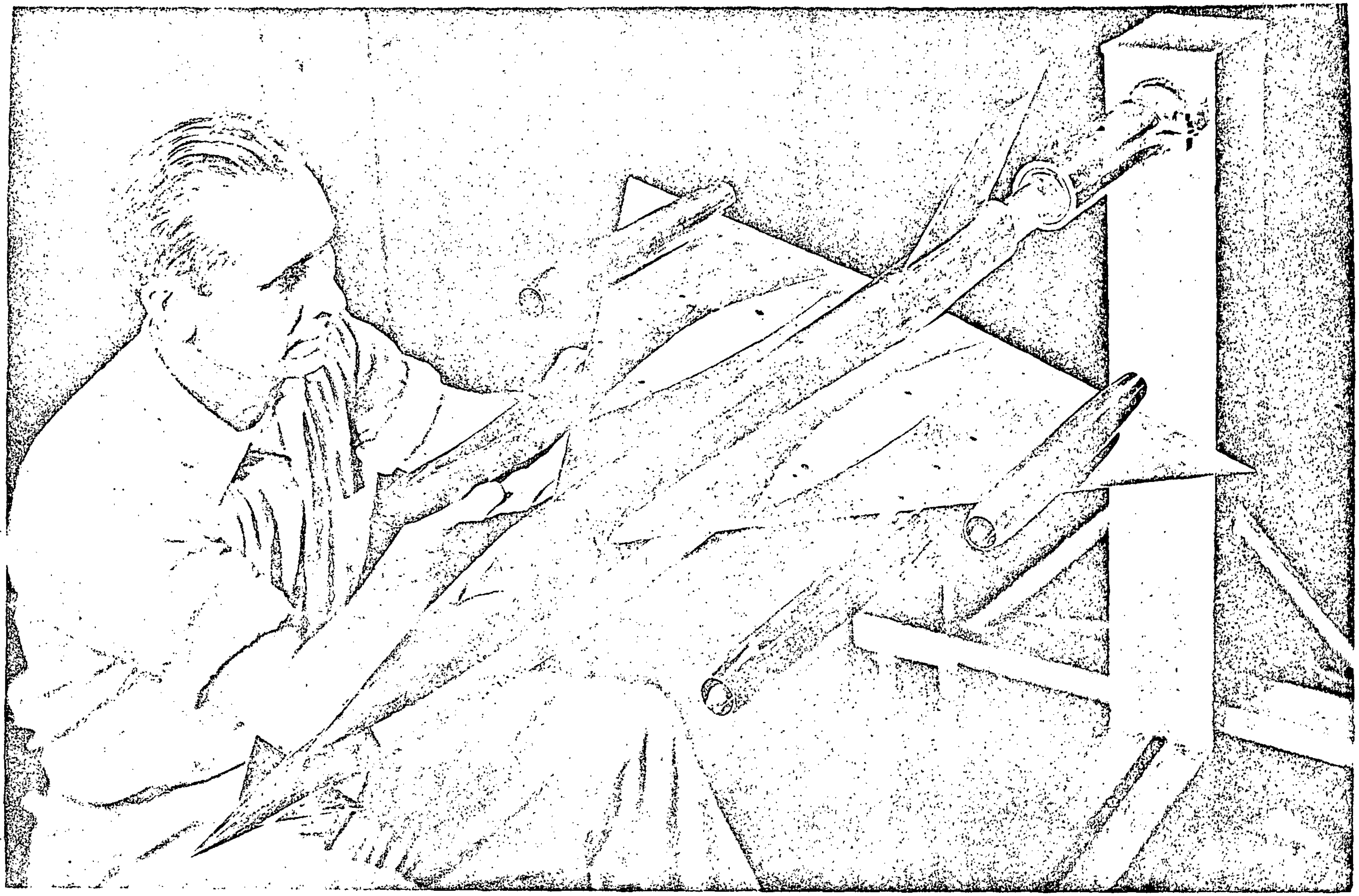

Figure 1.- The composite model equipped with split nacelles.

NACA
A-17987

[redacted]

Wing section	NACA 0004.5-64
Wing span in chord plane, inches	31.02
Wing area in chord plane, square inches	416.55
Wing mean aerodynamic chord, inches	17.91
Aspect ratio	2.3

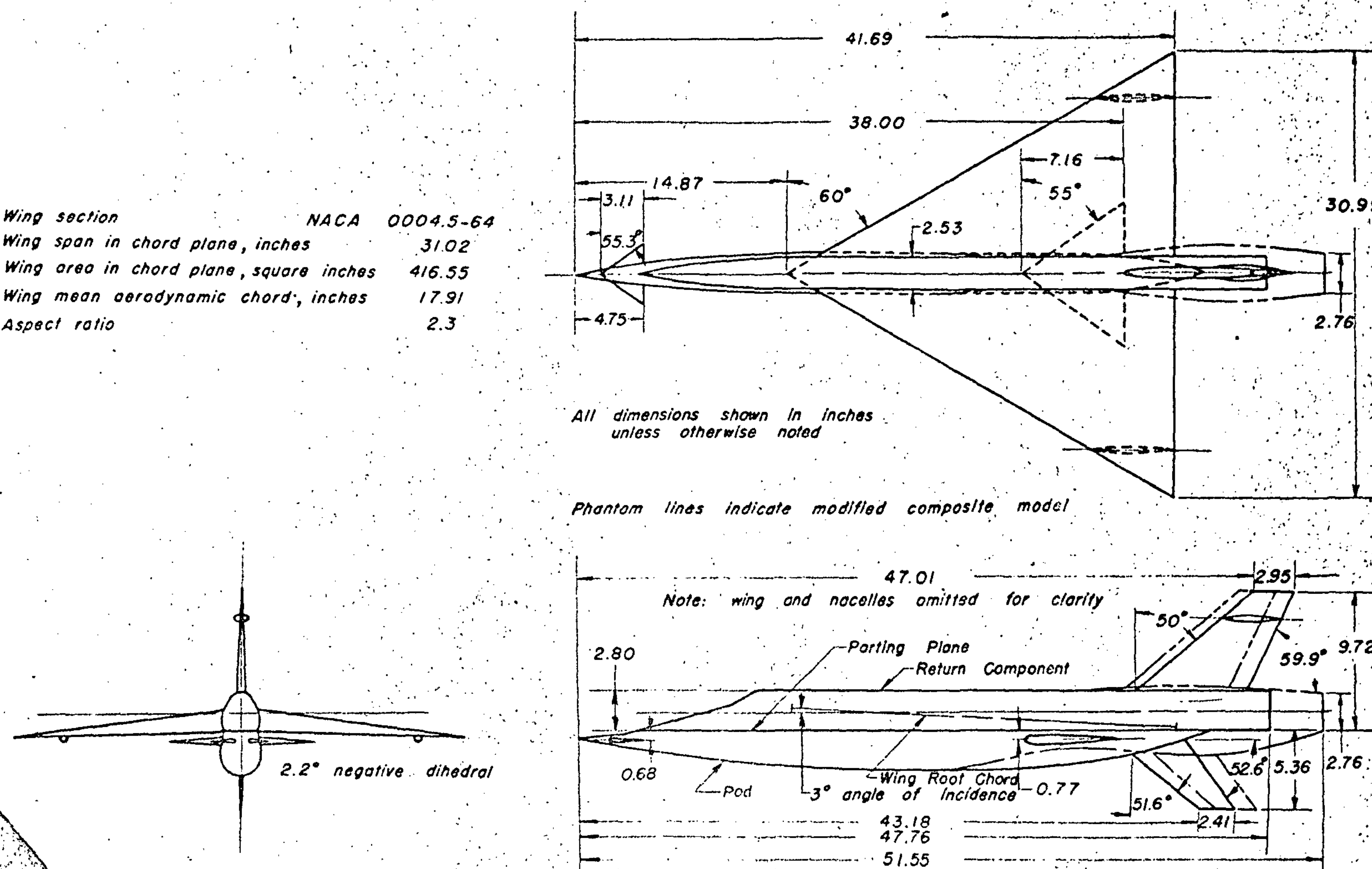

Figure 2.—Three-view drawing of the model.

[redacted]

[redacted]
SECURITY INFORMATION

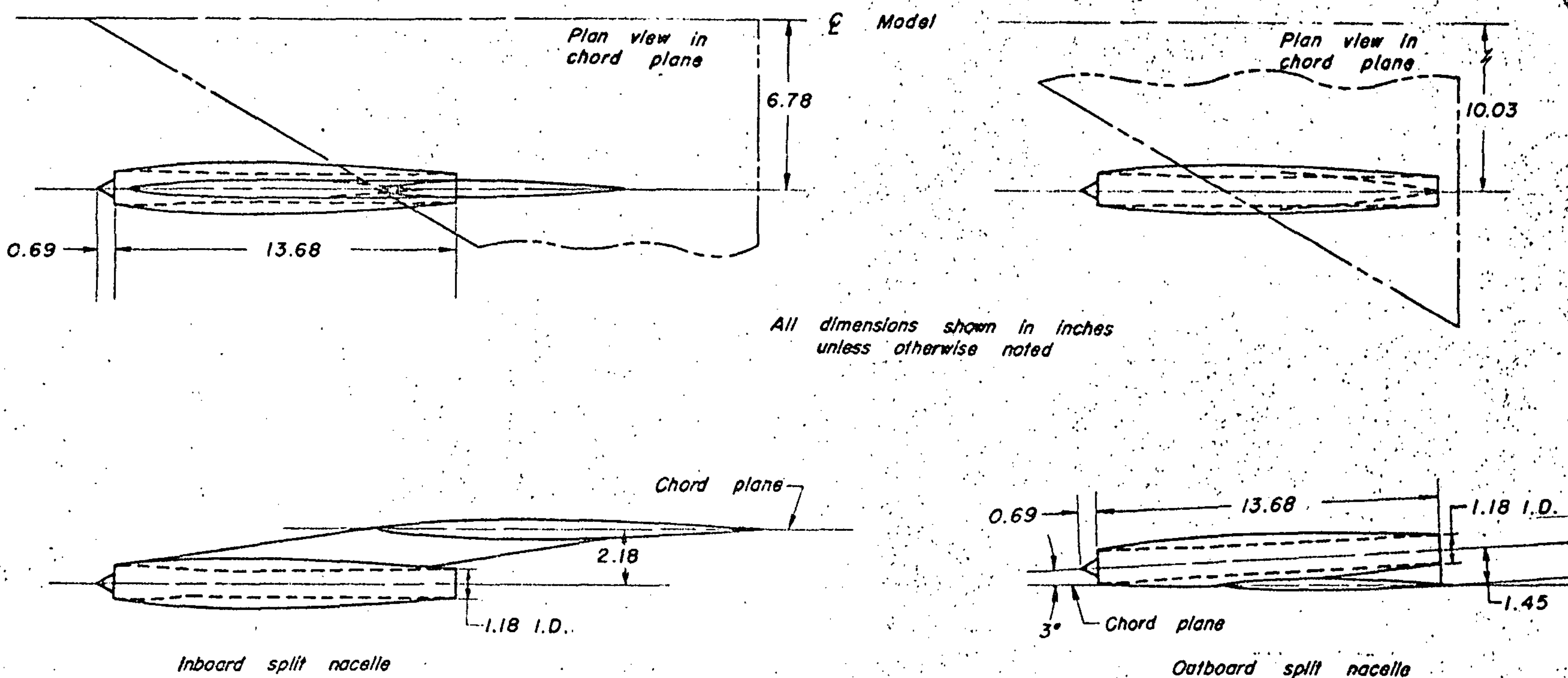

(a) Split nacelles.

Figure 3.—Details of the various nacelle configurations used on the model.

A6-63

[redacted]
SECURITY INFORMATION

9

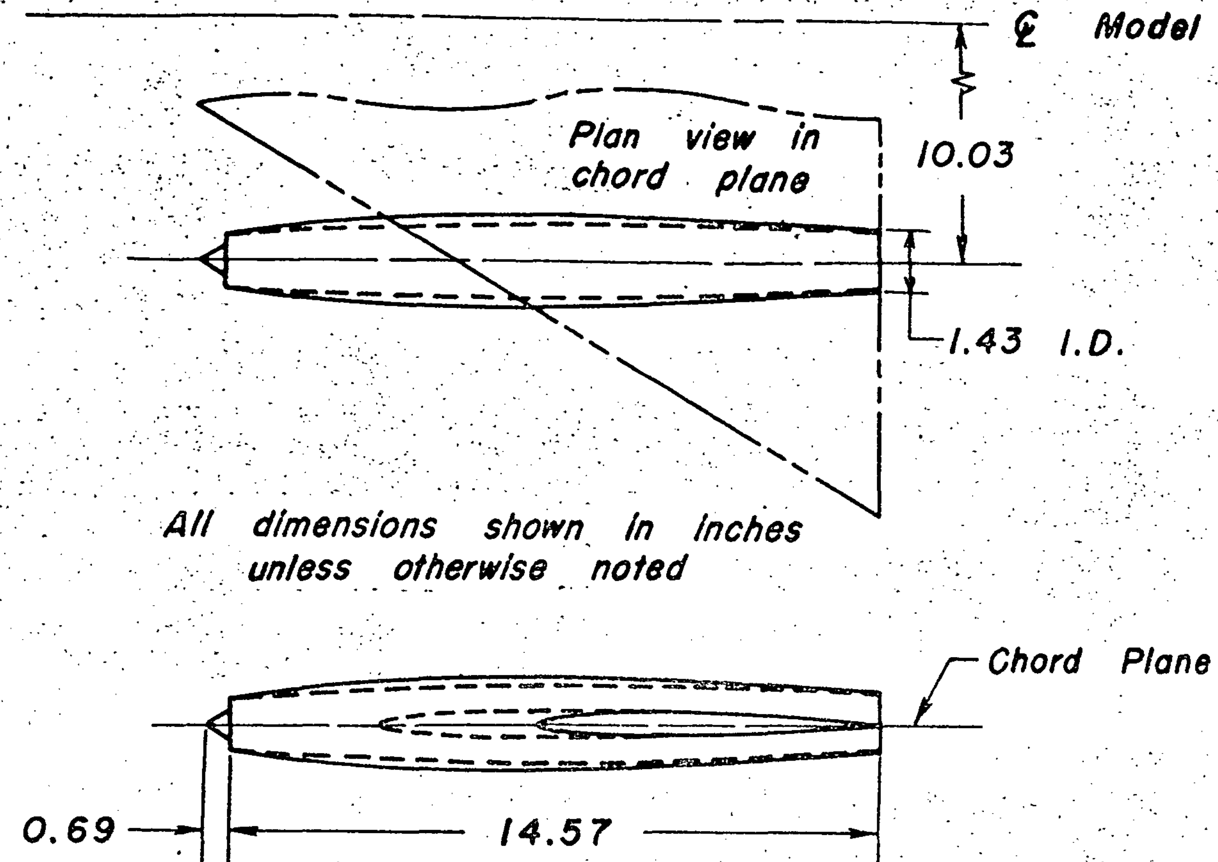

National Advisory Committee for Aeronautics,
Ames Aeronautical Laboratory,
Moffett Field, Calif.

(b) Outboard split nacelle on chord plane.

Figure 3.- Continued.

[redacted]

SECURITY INFORMATION

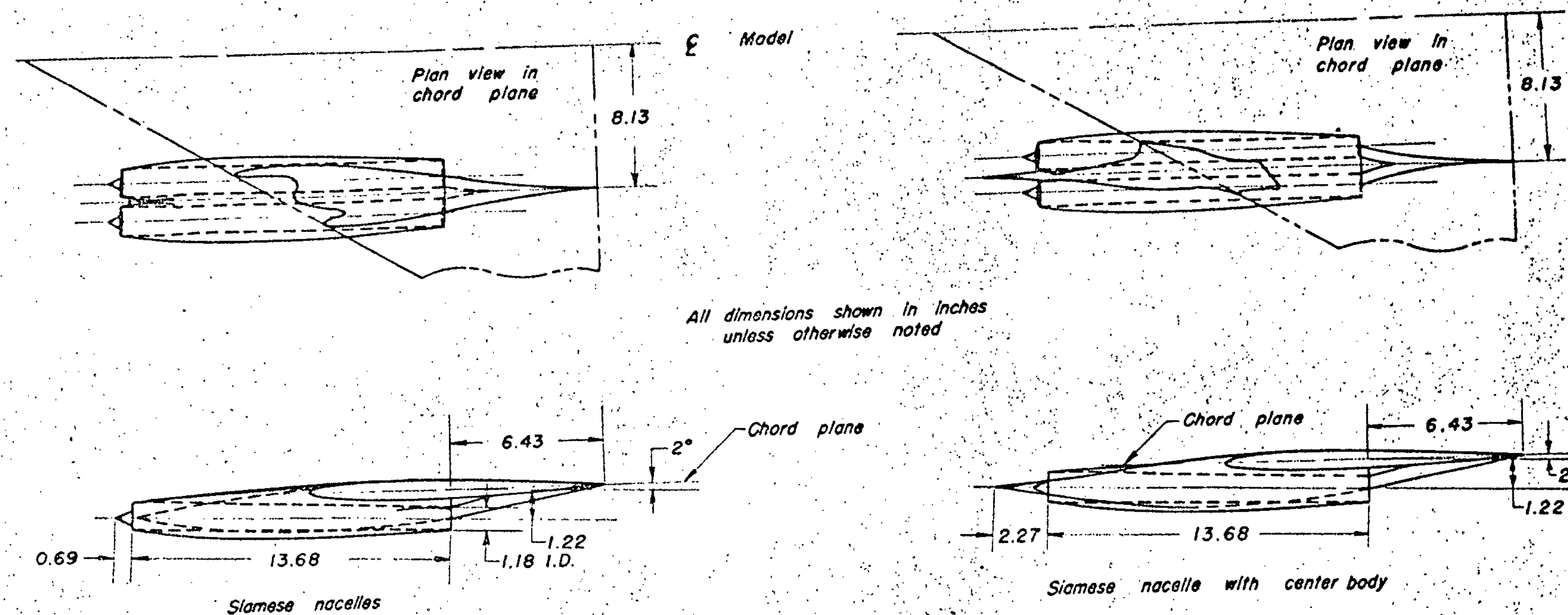

(c) Siamese nacelles.

Figure 3.– Concluded.

A6-63

NACA RM SA53C03

[redacted]

SECURITY INFORMATION

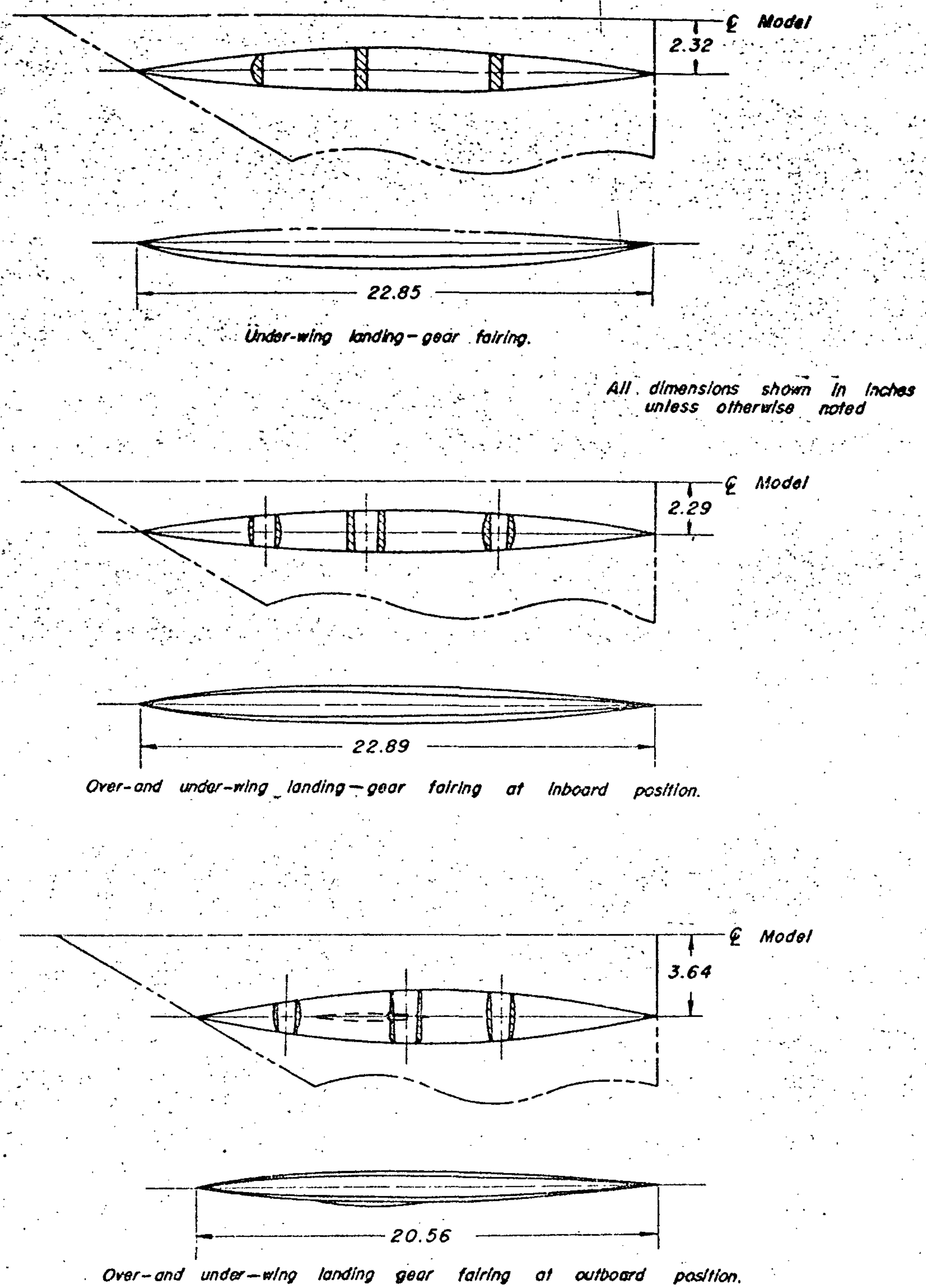

Figure 4.—Details of the landing-gear fairings used on the model.

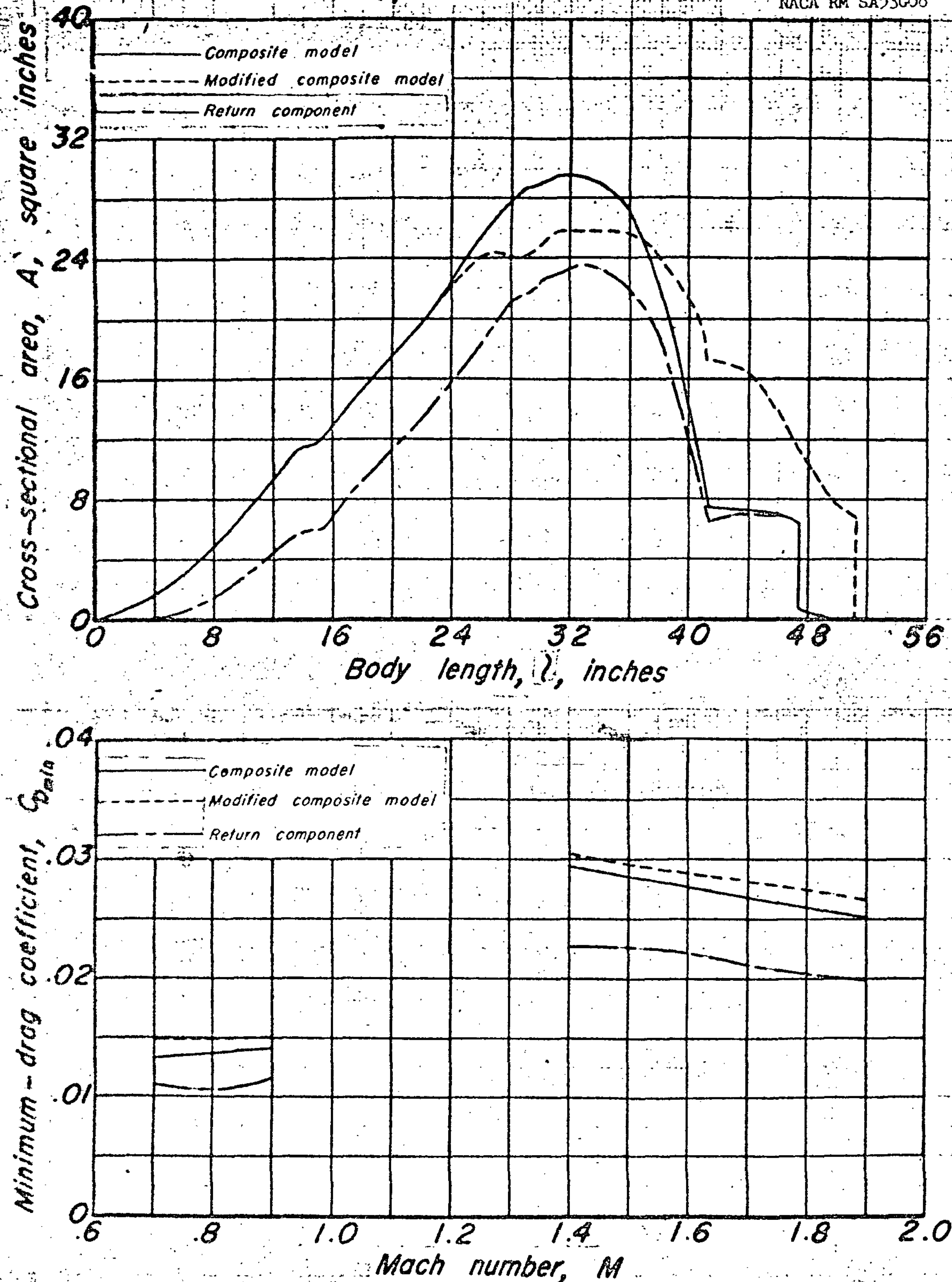

Figure 5.—The effect of longitudinal cross-sectional-area distribution upon the minimum-drag characteristics of the model with split nacelles. Reynolds number, 3.0 million.

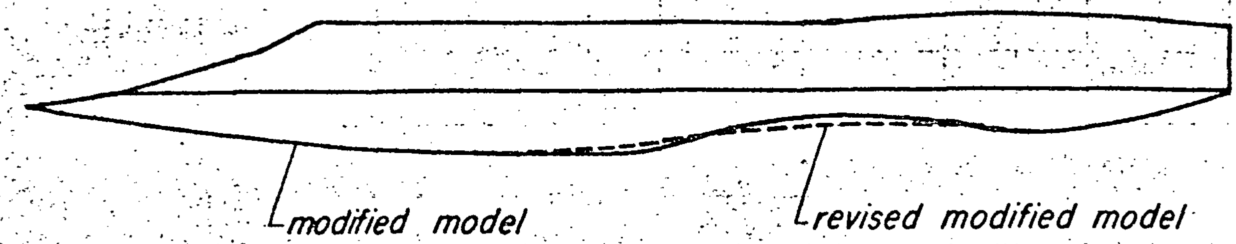

Side View

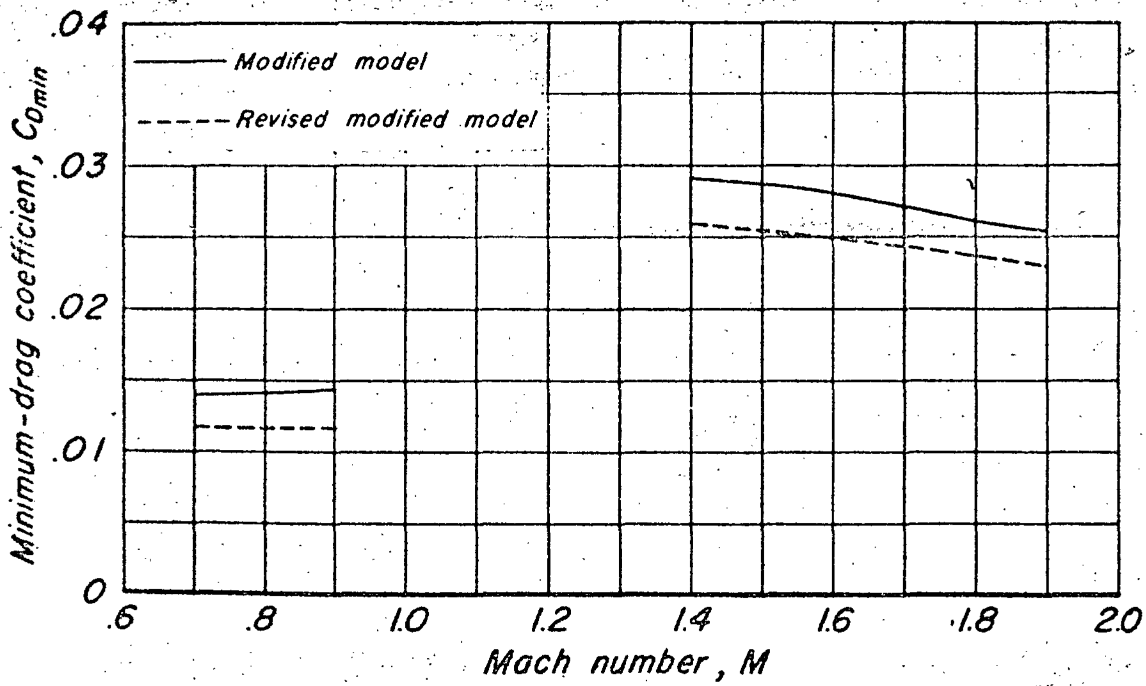

Figure 6.- A comparison of the minimum-drag characteristics of the modified and revised modified composite models without pod surfaces. Reynolds number, 3.0 million.

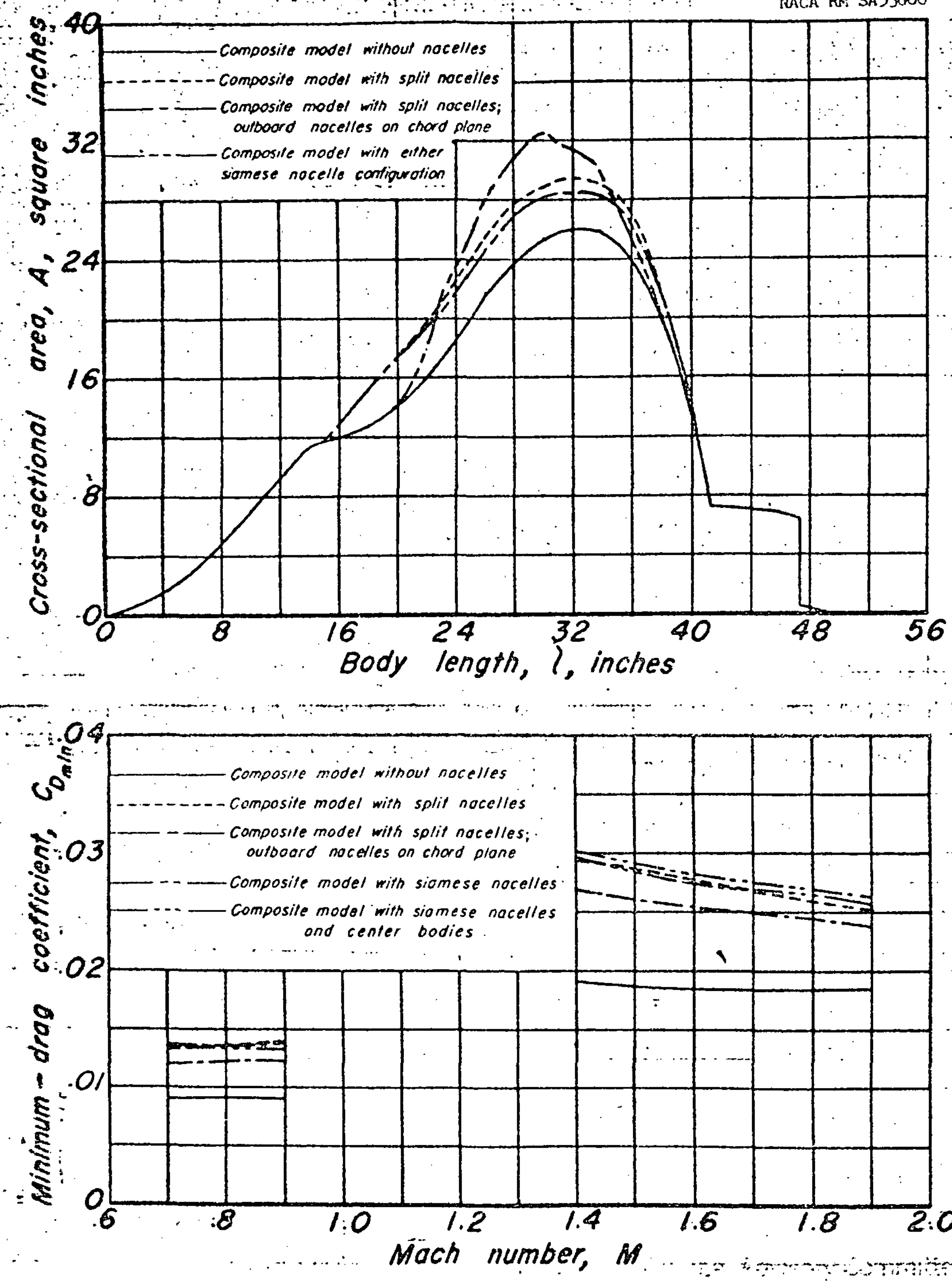

Figure 7.—Comparisons of the longitudinal cross-sectional-area distributions and the minimum-drag characteristics for the composite model with several nacelle configurations. Reynolds number, 3.0 million.

[redacted]

Restriction/Classification Cancelled

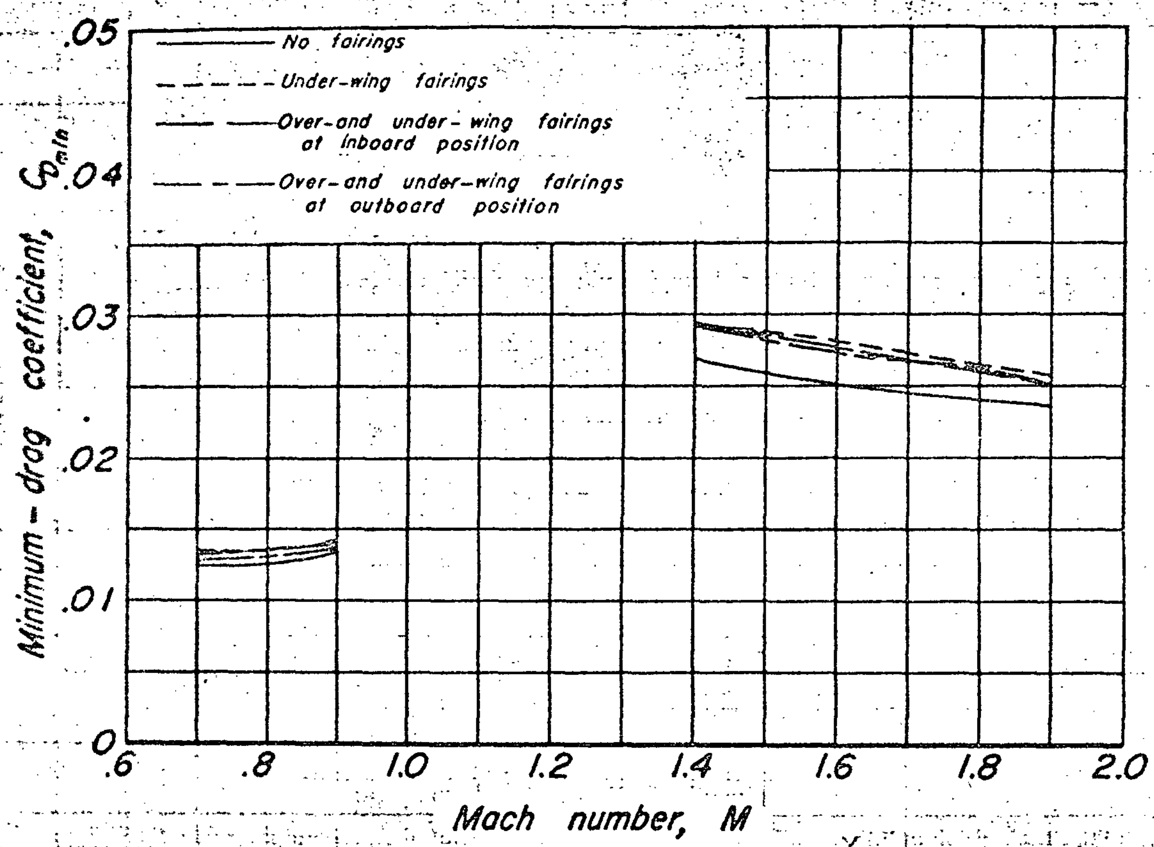

Figure 8.—The effect of several landing-gear fairings upon the minimum-drag characteristics of the composite model with split nacelles. Reynolds number, 3.0 million.

[redacted]

Restriction/Classification Cancelled

[redacted]

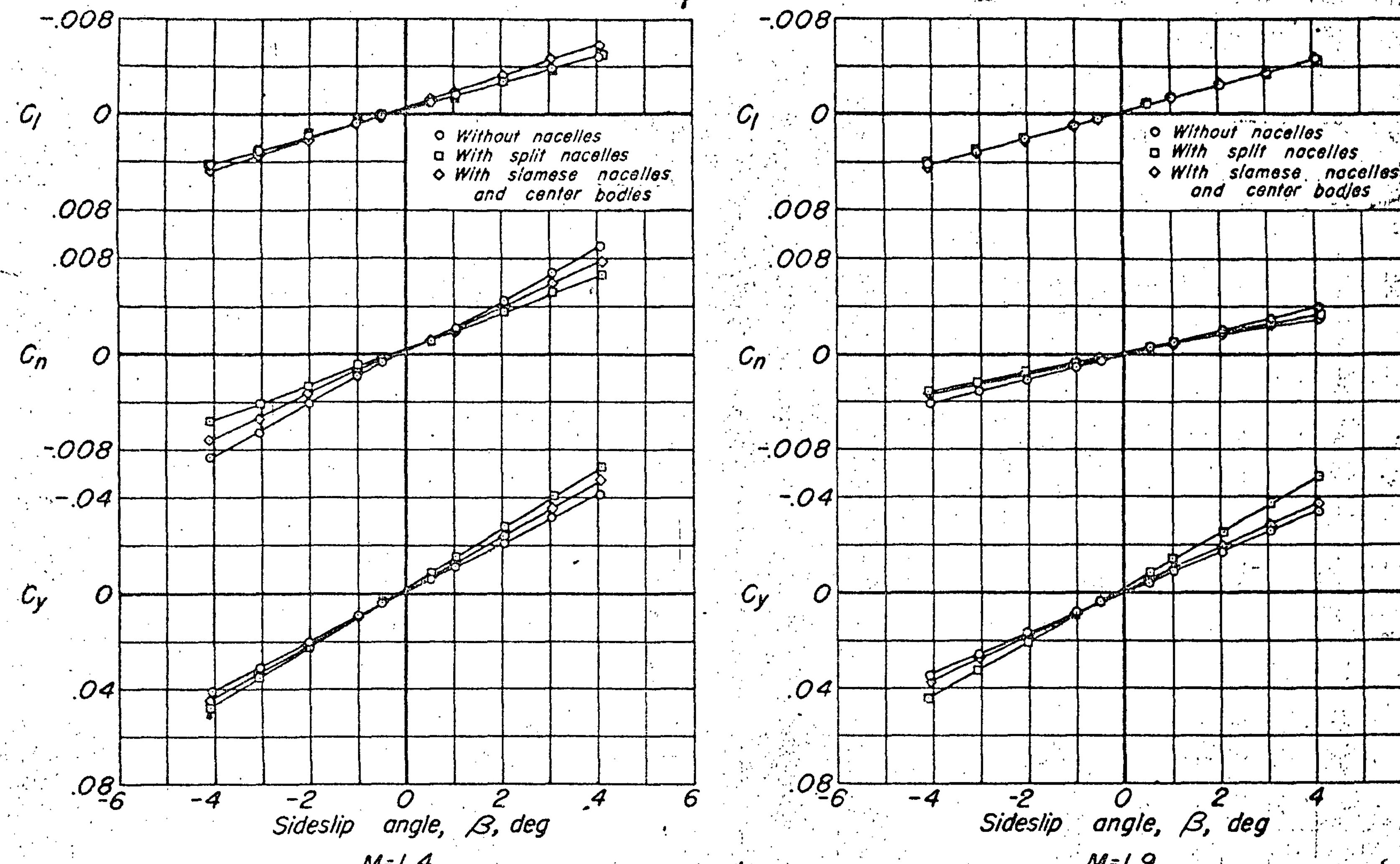

Figure 9.—Variation of the lateral-stability characteristics with sideslip angle for various nacelle configurations on the composite model at a lift coefficient of 0.08. Reynolds number, 3.0 million.

[redacted]